

Machine Learning of Time Series Using Time-delay Embedding and Precision Annealing

Alexander J. A. Ty, Zheng Fang, Rivver A. Gonzalez,

Department of Physics

University of California, San Diego

9500 Gilman Drive

La Jolla, CA 92093-0357

Paul. J. Rozdeba,

Institut für Mathematik

Universität Potsdam,

Karl-Liebknecht-Str. 24-25, 14476 Potsdam, Germany

and

Henry D. I. Abarbanel

Department of Physics

and

Marine Physical Laboratory (Scripps Institution of Oceanography)

University of California, San Diego

9500 Gilman Drive

La Jolla, CA 92093-0357

June 18, 2019

Abstract

Tasking machine learning to predict segments of a time series requires estimating the parameters of a ML model with input/output pairs from the time series. We borrow two techniques used in statistical data assimilation in order to accomplish this task: (1) time-delay embedding to prepare our input data, and (2) precision annealing as a training method. The precision annealing approach identifies the global minimum of the action ($-\log[P]$). In this way we are able to identify the number of training pairs required to produce good generalizations (predictions) for the time series. We proceed from a scalar time series $s(t_n); t_n = t_0 + n\Delta t$ and using methods of nonlinear time series analysis show how to produce a $D_E > 1$ dimensional time delay embedding space in which the time series has no false neighbors as does the observed $s(t_n)$ time series. In that D_E -dimensional space we explore the use of feed forward multi-layer perceptrons as network models operating on D_E -dimensional input and producing D_E -dimensional outputs.

1 Background

Machine learning methods for capturing the structure of a time series with the goal of predicting future segments of that time series have been analyzed for many years (Frank, Davey, & Hunt, 2001; Kajitani, Hipel, & McLeod, 2005; Goodfellow, Bengio, & Courville, 2016) . We revisit this problem using analysis tools allowing one to explore questions such as: if we are given a time series data set and a network architecture with which to predict a future segment of the time series, how many distinct samples of input/output pairs used in training the network are required to achieve very good prediction (generalization)? Ascertaining the number of training examples in order to attain a given performance metric, classification error for example, have been limited to the study of learning curves in the current ML literature.

In (Abarbanel, Rozdeba, & Shirman, 2018) two of the present authors recognized for the first time the equivalence between supervised machine learning (ML) and statistical data assimilation (SDA) as widely utilized in large Physics, Geophysical, and Biophysical modeling. This recognition opens up a variety of opportunities to use methods from SDA in tasks asked of ML with the possibility of both improving the performance of ML solutions as well as gaining insight as to how these solutions work. This paper builds on (Abarbanel et al., 2018) using our knowledge of how variational principles in ML may be implemented using methods not often practiced in that literature. Another of the insights in (Abarbanel et al., 2018) that we called ‘deepest learning’ when the number of layers in ML networks becomes continuous will be further visited in future publications (Abarbanel & Durstewitz, Fall, 2019).

We work within a setting where we are presented with scalar time series data $s(t_n) = s(t_0 + n\Delta t) = s(n)$, sampled every Δt . A sample of these data is shown in Fig. (1). We wish to present segments of these data to a multi-layer perceptron network and train the network to learn subsequent segments of the time series. The task asked of the network in this paper is to predict one step forward in time, namely $s(n + 1)$ given $s(n)$. There is no barrier to training this class of network to answer other questions about the data series. To train the selected network using the given data, we use a precision annealing (PA) method (Ye, Kadakia, Rozdeba, Abarbanel, & Quinn, 2014; Ye et al., 2015).

In this paper we explore the ability of a feed forward multi-layer perceptron (MLP) to accomplish learning this task. We show how PA allows us to answer questions about how many input/output pairs are required to achieve good generalization, namely, allowing the trained network to reliably predict from inputs not seen in the network training phase. In cases where there are practical limitations to the number of training data are available, (e.g. cost, ethical considerations, rarity, etc.) it is of interest to determine this. Our networks have only a few hidden layers, though there seems to be no barrier to making the network much deeper. The method we present can be used with other network architectures, for example, recurrent networks, with no fundamental change in approach. We address this configuration in the later parts of this paper.

2 Preparing the Data

We are presented with a time series, part of which is shown in Fig. (1). The data set is comprised of a large number of data values uniformly sampled in time

at times $t_n = t_0 + n\Delta t$. We do not know Δt . We are not given any further information about the sequence $\{s(n); n = 0, 1, \dots, N\}$. We were given $\approx 10^5$ data points, and we discarded about 10^4 of them to eliminate potential ‘transients’. Only 2048 of the data points are shown in Fig. (1).

Our goal here is to train a feedforward MLP network architecture to give as output $s(n+1)$ when presented with input $s(n)$. We could have used the method described here to train the network to predict $s(n+K)$ for any integer $K \geq 1$; we restrict our discussion here to $K = 1$. For larger values of K , extra caution would be required to assure that K is not so large that the input and output are not correlated.

Without further knowledge of the signal $s(n)$, we assume that although it is a sequence of scalars, it might have come from projection onto the s -axis from the operation of a higher dimensional dynamical system. To examine this we seek a ‘proxy space’ which carries the essential properties of the original higher dimensional source of the observed signal $s(n)$. For this purpose we turn to techniques of nonlinear time series analysis (Abarbanel, 1996; Kantz & Schreiber, 2003).

3 Time-Delay Vectors

If the observed time series $s(n)$ comes from projecting onto the s -axis, then points which appear to be nearby in time $t_n = t_0 + n\Delta t$ may be neighbors due to the projection rather than due to the dynamics that moves the actual system of interest forward in time in a higher dimensional space. Nonlinear time series methods for unfolding the scalar time series (Aeyels, 1981a, 1981b; Takens, 1981)

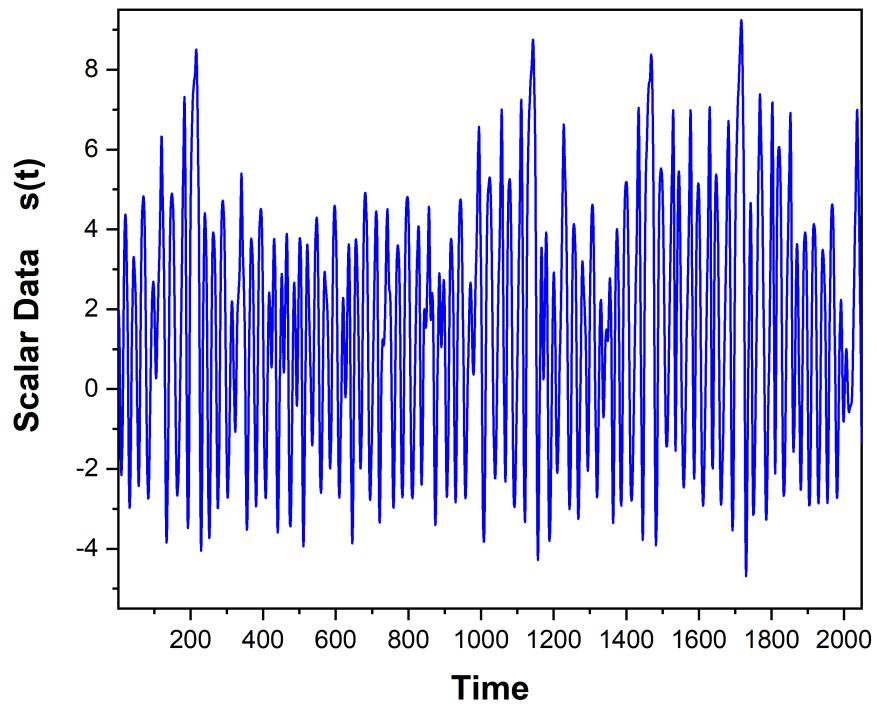


Figure 1: 2048 samples of the scalar data $s(t_n = t_0 + n\Delta t) = s(n)$ that comprise our data.

use the data $s(t_n) = s(n)$ along with the time delays of the data at time points $t_n + q\tau\Delta t = t_0 + (n + q\tau)\Delta t : s(n + q\tau)$. τ and q are integers.

The idea here is that $s(n + \tau)$ contains information on how the dynamics of the source of the time series $s(n) \rightarrow s(n + \tau)$ moves the system of interest forward in time. This information is not available in $s(n)$ alone.

This leads us to form the D_E -dimensional vector extending from each time t_n :

$$\mathbf{s}(n) = [s(n), s(n + \tau), s(n + 2\tau), \dots, s(n + (D_E - 1)\tau)], \quad (3.1)$$

or, in components,

$$S_q(n) = s(n + (q - 1)\tau); \quad q = 1, 2, \dots, D_E; \quad (3.2)$$

D_E is also an integer.

To use this idea in a practical sense, we must estimate the time delay τ and the dimension D_E of the vectors $\mathbf{S}(n)$ containing the properties of the original state space from which $s(n)$ is projected. The value of τ should not be too small or the system will not have revealed the new information coming from the operation of the underlying dynamics, and τ should also not be too large or noise and intrinsic instabilities of the (nonlinear) dynamics will erase the utility of information at time $n + (D_E - 1)\tau$.

3.1 Selecting τ

To estimate τ we use an information theoretic ‘correlation function’, the average mutual information (AMI) (Fano, 1961; Fraser & Swinney, 1986). This function

is nonnegative (Fano, 1961), and the Fraser (Fraser & Swinney, 1986) criterion is to select the first minimum of the AMI as a balance between τ being too large or too small. The minimum means that the coordinates $s(n)$ and $s(n + \tau)$ are correlated, but not so strongly correlated that no new information on the origin of the time series results from knowing both $s(n)$ and $s(n + \tau)$.

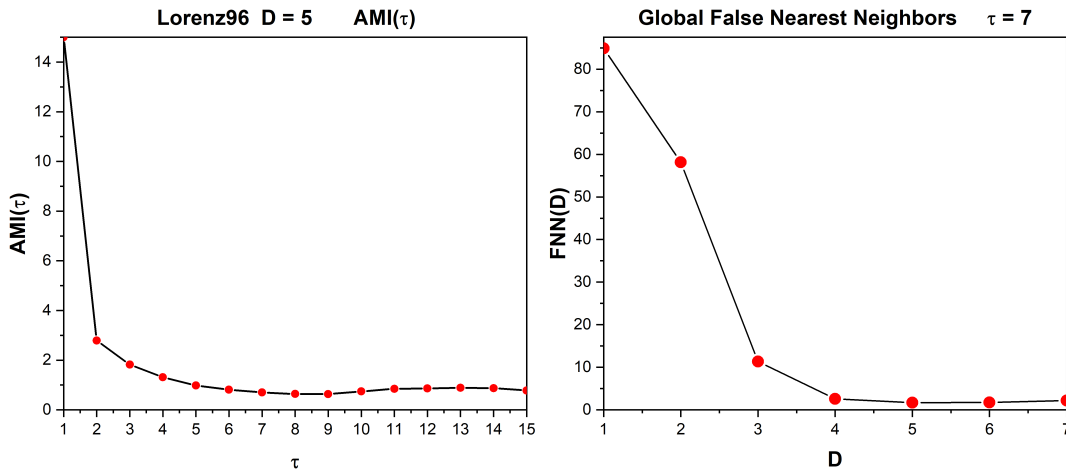


Figure 2: **Left:** Average Mutual Information Eq. (3.3), $AMI(\tau)$ between $s(n)$ and $s(n + \tau)$ as a function of the time delay τ . Using the Fraser (Fraser & Swinney, 1986) criterion, we select the first minimum near $\tau \approx 7 - 8$ for a useful time delay. **Right:** The false nearest neighbor criterion for selecting a global embedding dimension D_E for vectors whose components are separated by the time delay τ using $AMI(\tau)$.

$AMI(\tau)$ requires the joint distribution of $\{s(n), s(n + \tau)\}$, $P(s(n), s(n + \tau))$, as well as $P(s(n))$ and $P(s(n + \tau))$. The latter come from the marginal distributions of $P(s(n), s(n + \tau))$.

$$AMI(\tau) = \sum_{\{s(n), s(n + \tau)\}} P(s(n), s(n + \tau)) \log \left[\frac{P(s(n), s(n + \tau))}{P(s(n)) P(s(n + \tau))} \right]. \quad (3.3)$$

This quantity, $AMI(\tau)$, answers the question: how much information (in bits if the logarithm is to base 2) do we learn from $s(n)$ about $s(n + \tau)$ on the average over all joint values of $\{s(n), s(n + \tau)\}$.

In the Left Panel of Fig. (2) we display $AMI(\tau)$ evaluated from 2^{15} samples of the time series of $s(n)$. The first minimum of this is near $\tau \approx 7$ or 8.

3.2 Selecting D_E

Once τ has been selected, the estimation of D_E is made by systematically asking when neighbors in dimension D for $\mathbf{S}(n)$ remain neighbors when $\mathbf{S}(n)$ is expressed in dimension $D + 1$. This method of false nearest neighbors reveals a global property of the source of the time series; namely, the minimum dimension D_E within which the vectors $\mathbf{S}(n)$ can represent trajectories that contain no neighbors arriving through projection from higher dimensions. The analysis of these global false nearest neighbors $FNN(D)$ is shown in the **Right Panel** of Fig. (2) where $\tau = 7$ is used. It is good to check that our results are robust against selecting $\tau = 7$; using $\tau = 6$ or $\tau = 8$ each yield $D_E = 5$. This is discussed in (Abarbanel, 1996) in more detail.

Using $D_E = 5$, we can evaluate the Lyapunov exponents of the dynamical system at the source of the data $s(n)$. The methods for doing this are described in (Abarbanel, 1996; Kantz & Schreiber, 2003). Briefly summarized: one uses the development of trajectories in the D_E -dimensional space, and following a few trajectories nearby each other in this space from one location in space to another construct a local map from one set of points to the location where they go in one step. This permits one to read off the local Jacobian matrix step by step through out the trajectories in D_E -dimensional space. According to the Oseledec

theorem (Abarbanel, 1996) the sequential products of these $D_E \times D_E$ matrices when diagonalized yields the Lyapunov exponents. To accurately estimate all D_E Lyapunov exponents, one uses a recursive **QR** decomposition.

Following this protocol, we find two positive exponents. There is one zero exponent telling us that the source of the data is some (unknown) differential equation for five state variables. There are two negative exponents. The sum of the Lyapunov exponents is negative, and the associated information dimension of the attractor is about 4.4 (Abarbanel, 1996; Kantz & Schreiber, 2003).

Until this point, we have withheld information about the method in which the data was generated for this experiment. We now reveal that it is a $D = 5$ Lorenz 96 model with forcing term $F = 8.15$. Information was kept from the reader in order to illustrate that in order to perform such an analysis, information about the original system is not required.

Now that we have established estimates for τ and D_E , we want to use the observed time evolution $\mathbf{S}(n) \rightarrow \mathbf{S}(n + 1)$ to train a network to implement this discrete time map in D_E -dimensions.

4 Training a Selected Neural Network

The idea is now to work in $D_E = 5$ dimensional space on vectors $\mathbf{S}(n) = [s(n), s(n + \tau), s(n + 2\tau), \dots, s(n + (D_E - 1)\tau)]$, and build a machine that learns the discrete time mapping $\mathbf{S}(n) \rightarrow \mathbf{S}(n + 1)$.

To the scalar data $\mathbf{s}(n)$ we add noise of mean zero and rms error σ to form noisy scalar data $y(n) = s(n) + \text{Noise}(0, \sigma)$. In our calculations we selected σ to be 2% of the dynamical range of the observed data. With higher noise levels, the

information content of each individual training pair is reduced, leading to a need of additional training pairs to achieve similar prediction capabilities.

Using these noisy scalar data we form a data library of many input/output D_E -dimensional vector pairs to be used at the input port at layer l_0 and the output port at layer l_F , to train a neural network. We use $k = 1, 2, \dots, M$ members of this library as our training set.

$$\mathbf{Y}^{(k)}(l_0) = \{y(k), y(k + \tau), y(k + 2\tau), y(k + 3\tau), y(k + 4\tau)\}, \quad (4.1)$$

$$\mathbf{Y}^{(k)}(l_F) = \{y(k + 1), y(k + 1 + \tau), y(k + 1 + 2\tau), y(k + 1 + 3\tau), y(k + 1 + 4\tau)\},$$

$k = 1, 2, \dots, M$ here and $D_E = 5$.

The network we choose is a Multi-layer Perceptron, and we wish to train it to take at the input vectors $\mathbf{Y}^{(k)}(l_0; n)$ and produce at the output vectors $\mathbf{Y}^{(k)}(l_F; n)$. At the input layer l_0 we have **one** input port with D_E slots. At the output layer l_F we have **one** output port with D_E slots. The network has $l_F - 2$ hidden layers $l = \{l_1, l_2, \dots, l_F - 1\}$. At the hidden layers we have D_{hl} active units ('neurons') at layer l .

As a function of the three quantities $\{l_F, D_{hl}, M\}$: l_F , the number of layers or the 'depth' of the network; D_{hl} , the number of active units in layer l or the breadth of the network; and M , the number of distinct input/output pairs containing the information presented to the network for training, we wish to analyze, using statistical Physics methods, the quality of the training, the accuracy of the operation of the trained network on input/output pairs **not** used in training, and the ability of the trained network to represent the information in the M data pairs. In the networks we develop here, we take D_{hl} to be independent of l .

4.1 The Action

In much of machine learning one seeks to minimize a cost function evaluated at the input and the output layers of a selected network. We call the activity variables (‘neurons’) at layer l $x_q(l)$ for active unit $q = 1, 2, \dots, D_{hl}$ in layer l . The cost function for each input/output pair is at time k

$$C(k) = \frac{R_m}{2} \frac{1}{D_{h0} + D_{hf}} \left[\sum_{q=1}^{D_{h0}} (x_q^{(k)}(l_0) - y(k + (q-1)\tau))^2 + \sum_{q=1}^{D_{hf}} (x_q^{(k)}(l_F) - y(k + 1 + (q-1)\tau))^2 \right], \quad (4.2)$$

where the noise or errors in the input and output data have been taken to be Gaussian with zero mean and diagonal precision matrix R_m . $D_{h0} = D_{hf} = D_E$ for us.

This is to be minimized subject to a layer-to-layer connection rule

$$x_q(l+1) = f_q \left(\sum_{v=1}^{D_{hl}} \mathbf{W}(l)_{qv} x_v(l) \right) \quad q = 1, \dots, D_{h(l+1)}, \quad (4.3)$$

with $\mathbf{W}(l)$ a matrix of weights to be determined in the minimization of $C(k)$.

If Gaussian errors with precision matrix R_f are accepted in the layer-to-layer rule Eq. (4.3), then the full cost function is

$$A(x(l); k) = C(k) + \frac{R_f}{2} \frac{1}{\sum_{l=l_1}^{l_F} D_{hl}} \sum_{l=l_0}^{l=l_F} \sum_{q=1}^{D_{h(l+1)}} \left(x_q^{(k)}(l+1) - f_q \left(\sum_{v=1}^{D_{hl}} \mathbf{W}(l)_{qv} x_v^{(k)}(l) \right) \right)^2,$$

and we call this the ‘action’, after its usage in statistical Physics, for a single input/output data pair chosen at time k .

When we have many input/output pairs, we add a label to the active states in the network $x_q(l) \rightarrow x_q^{(k)}(l)$, and our goal is to minimize the action

$$\begin{aligned}
A(x_q^{(k)}(l), \mathbf{W}(l)) &= \frac{1}{M} \sum_{k=1}^M \left\{ \frac{R_m}{2} \frac{1}{D_{h0} + D_{hf}} \left[\sum_{q=1}^{D_{h0}} (x_q^{(k)}(l_0) - y(k + (q-1)\tau))^2 \right. \right. \\
&\quad \left. \left. + \sum_{q=1}^{D_{hF}} (x_q^{(k)}(l_F) - y(k + 1 + (q-1)\tau))^2 \right] \right. \\
&\quad \left. + \frac{R_f}{2} \frac{1}{\sum_{l=l_1}^{l_F} D_{hl}} \sum_{l=l_0}^{l_F} \sum_{q=1}^{D_{h(l+1)}} \left(x_q^{(k)}(l+1) - f_q \left[\sum_{v=1}^{D_{hl}} \mathbf{W}(l)_{qv} x_v^{(k)}(l) \right] \right)^2 \right\}, \tag{4.4}
\end{aligned}$$

with respect to the connection weight matrices $\mathbf{W}(l)$ and the activities $x_q^{(k)}(l)$. Minimizing this action recognizes that for each input/output training pair, the activity of the network nodes may differ, but averaging over all M presentations of pairs from the library will train a possible generalizable network characterized by the $\mathbf{W}(l)$ and any other fixed parameters in the nonlinear functions f_q .

5 Use of the Action

The action $A(\mathbf{X})$, where \mathbf{X} is the collection of all $x_q^{(k)}(l)$ in the network as well as the $\mathbf{W}(l)$ and other fixed parameters, is proportional to the negative of the logarithm of the conditional probability of the full state \mathbf{X} conditioned on the M members of the input/output library, collected into a quantity \mathbf{Y} , used in the training set: $P(\mathbf{X}|\mathbf{Y}) \propto \exp[-A(\mathbf{X})]$. An important use of this conditional probability density is the evaluation of expected values of functions $G(\mathbf{X})$ on the

variables \mathbf{X} , and this is evaluated by doing the integral

$$E[G(\mathbf{X})|\mathbf{Y}] = \langle G(\mathbf{X}) \rangle = \frac{\int d\mathbf{X} G(\mathbf{X}) \exp[-A(\mathbf{X})]}{\int d\mathbf{X} \exp[-A(\mathbf{X})]} \quad (5.1)$$

It is here that the connection of machine learning with statistical Physics becomes apparent.

Estimating this integral can always be done with various Monte Carlo methods, and depending on the action $A(\mathbf{X})$ surfaces in \mathbf{X} may be accomplished by finding the maxima of $P(\mathbf{X}|\mathbf{Y})$, or equivalently the minima of $A(\mathbf{X})$. The latter method (Laplace, 1774, 1986) is why we are interested in the paths \mathbf{X} which yield minima of $A(\mathbf{X})$.

6 Precision Annealing

We have developed a precision annealing (PA) approach (Ye et al., 2014, 2015) for the minimization of the action Eq. (4.4) directed to finding the path with the smallest value of the action. The problem of finding the global minimum of the action, a nonlinear objective function of \mathbf{X} , is NP-complete (Murty & Kabadi, 1987). PA is a continuation method (Allgower & Georg, 1990) in R_f that begins at very small R_f where the global minimum is a solution to minimizing a quadratic form; this can be done in a straightforward manner, and moves adiabatically in R_f to quite high values. Formally as $R_f \rightarrow \infty$, the layer-to-layer rule used in constructing the network becomes precise and deterministic.

While we have no mathematical proof that the global minimum is found, our numerical results indicate this may be the case. The PA method produces a set of

minima of the action giving a numerical clue as to the roughness of the surface in path \mathbf{X} space. It also finds low magnitude action minima with much higher rates of success than starting directly with large R_f .

The action surface $A(\mathbf{X})$ depends, among other items, on the number of measurement pairs M , on the hyper-parameter R_f , and on the number of model layers between l_0 and l_F . As the number of hidden layers increases, the model architecture deepens.

$$R_f \ll 1 ;$$

Choose \mathbf{X}^0 from a uniform distribution for each N_I ;

while *no individual $A(X')_{N_I}$ is substantially less than the group of A* **do**

foreach N_I **do**

 Minimize $A(\mathbf{X})$ using \mathbf{X}^0 as an initial guess;

 Arrive at \mathbf{X}' ;

$\mathbf{X}^0 = \mathbf{X}'$;

 Update $R_f = R_f * \alpha$;

end

end

Algorithm 1: Precision() annealing algorithm

At the first step of PA we choose a solution to the optimization problem at $R_f = 0$ and select the states at the hidden layers as drawn from a uniform distribution with ranges known from the dynamical range of the input/output state variables. One can learn that dynamical range well enough by solving the underlying model forward for various initial conditions. We make this draw N_I times, and now have N_I paths \mathbf{X}^0 as candidates for the PA procedure.

Now we select a small value for R_f , call it R_{f0} , and use the previous N_I

paths \mathbf{X}^0 as N_I initial choices in our minimization algorithm. After using that minimization procedure we find N_I new paths \mathbf{X}^1 for the minimization problem with $R_f = R_{f0}$. This gives us N_I values of the action $A(\mathbf{X}^1)$ associated with the new paths \mathbf{X}^1 .

Next we increase the value of R_f to $R_f = R_{f0}\alpha$ where $\alpha > 1$. For this new value of R_f , we perform the minimization of the action starting with the N_I initial paths \mathbf{X}^1 from the previous step to arrive at N_I new paths \mathbf{X}^2 . Evaluating the action on these paths $A(\mathbf{X}^2)$ now gives us an ordered set of actions that are no longer as degenerate. Many of the paths \mathbf{X}^2 may give the same numerical value of the action. However, typically the ‘degeneracy’ lies within the noise level of the data $\approx (1/\sqrt{R_m})$.

This procedure is continued until R_f is ‘large enough’ which is indicated by at least one of the action levels becoming substantially independent of R_f and typically smaller than the others.

Effectively PA starts with a problem ($R_f = 0$) where the global minimum is apparent and systematically tracks it and many other paths through increases in R_f . In doing the ‘tracking’ of the global minimum, one must check that the selected value of α is not too large lest one leave the global minimum and land in another minimum. Checking the result using smaller α is always worthwhile.

It is important to note that simply starting with a large value of R_f , $R_f \approx 1$ or larger, places one in the undesirable situation of the action $A(\mathbf{X})$ having multiple local minima into which any optimization procedure is quite likely to fall.

In the dynamical problems we have examined, one typically finds that as the number of measurement pairs M is increased, more terms are added in the sum in Equation 4.4, thus raising the action levels of minima disproportionately until

there is one dominant minimum. This we attribute to the additional information from the augmented set of measurement pairs.

6.1 Smallest Minimum; Not Necessarily a Convex Action

As our goal is to provide accurate estimations of the conditional expected value of functions $G(\mathbf{X})$ Eq. (5.1) where \mathbf{X} , a path in model space, is distributed as $\exp[-A(\mathbf{X})]$, we actually do not require convexity of $A(\mathbf{X})$ as a function in path space. From the point of view of accurately estimating expected values, it is sufficient that the lowest action level be **much** smaller than the second lowest action level. If the action value at the lowest level $A(\mathbf{X}_{\text{lowest}})$ is much smaller than the action value at the next minimum $A(\mathbf{X}_{\text{second lowest}})$, then by a factor $\exp[-\{A(\mathbf{X}_{\text{lowest}}) - A(\mathbf{X}_{\text{second lowest}})\}]$, the lowest path $\mathbf{X}_{\text{lowest}}$ dominates the integral to be done and provides a sensible choice for the path at which to evaluate the integral.

We will see in the examples below that when the PA procedure is used we may encounter situations where the action is apparently not convex. However, it may have a distinct smallest action level, much smaller in magnitude than the next lowest action level. That lowest level is expected to give a path which gives an accurate estimation to the expected value of functions $G(\mathbf{X})$. This may occur in cases where sufficient information from the data has been transferred to the model, and this can indicate the size model adequate for the problem posed.

7 Action Levels for Our Time Series $\{s(n)\}$

We will now build and train a feedforward MLP (Rozdeba, 2018) to learn the function $s(n) \rightarrow s(n+1)$ using D_E -dimensional data pairs from our library. We examined networks with $D_E = 5$ dimensional input (l_0) and output (l_F) layers and 1-5 hidden layers each with the same number D_h of active units (‘neurons’). The nonlinear function operating from layer-to-layer was chosen to be $\tanh(\bullet)$. We use the Python based program VarrAnneal (Rozdeba, 2018) to perform the minimization of the action at each value of $R_f/R_m > 0$.

To prepare our data for these network choices, we first scaled all of the noisy inputs $y(n)$ to lie within the range $[-1, 1]$ via

$$y(n) \rightarrow \frac{2y(n) - (y_{max} + y_{min})}{y_{max} - y_{min}}, \quad (7.1)$$

where $y_{max, min}$ are the maximum and minimum values taken by the noisy data. These scaled values were used to construct our data library of input/output pairs.

7.1 Two Hidden Layers; $D_h = 15$; $M = 50, \dots, 1200$

Using PA and systematically moving R_f/R_m from $R_{f0}/R_m \approx 10^{-8}$ to $R_f/R_m \approx 10^{11}$ we evaluated $A(\mathbf{X})$ for $M = 50, 100, \dots, 1200$ input/output pairs. R_f was slowly increased using $\alpha = 1.1$. At each value of R_f/R_m we used $N_I = 20$ initializations of the PA procedure.

We first examine the structure of the action levels as a function of R_f/R_m for $M = 50, 300, 900, 1200$ I/O pairs. This is displayed in Fig. (3). Note that the action levels become nearly independent of R_f/R_m for large values of this

hyperparameter. Equally interestingly is the initial rise of $A(\mathbf{X})$ for large R_f/R_m as M increases. Then this saturates as the information in the time series $s(n)$ is represented fully in the network. See Fig. (4). Recall we call this the information content as, up to a constant $\langle A(\mathbf{X}) \rangle = \langle -\log[P(\mathbf{X})] \rangle$.

8 Errors in Training and Validation

Once we have trained the proposed network, we can evaluate its quality when performing the task we have set it. In the example we have discussed here, that task is summarized as: when presented with a D_E -dimensional vector of inputs, created from time delays of a signal $s(n)$, accurately produce the next element of the time series $s(n+1)$. The quantities $s(n)$ and $s(n+1)$ are the first components of the data vectors.

We have tested (or validated) the operation of the network both on the data used to train the network and on data held aside in our library of I/O pairs. The latter is often called the “test” set or validation set or prediction set portion of the total data available to us (Frank et al., 2001).

The error on the training set as a function of the number M of I/O pairs used to train the network is given as

$$MSE_{\text{Training Error}}(M) = \frac{1}{M} \sum_{k=1}^M \frac{1}{D_E} \sum_{q=1}^{D_E} (x_q^{(k)}(l_F) - y(k+1+(q-1)\tau))^2 \quad (8.1)$$

This compares, in a least squares sense, the D_E -dimensional output $x_q^{(k)}(l_F)$ from the trained network with the data from the **training** set, $y(k+1+(q-1)\tau)$, that are the output side of the input/output training pairs. The input to the

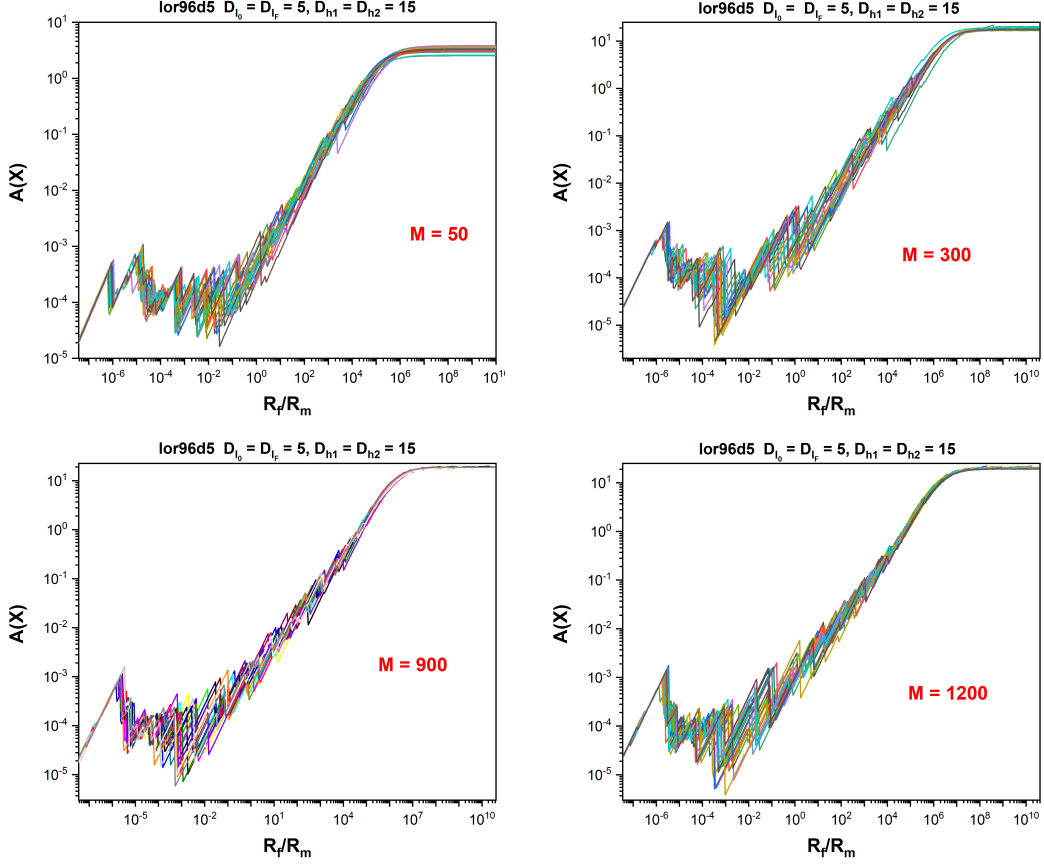


Figure 3: Action Levels as a function of R_f/R_m for the time series data $s(n)$ input into our two hidden layer MLP as a D_E dimensional data vector. The number of I/O pairs for these calculations were $M = 50, 300, 900, 1200$. $N_I = 20$ action levels associated with the N_I initializations of the optimization algorithm used at each value of R_f/R_m . In these calculations $\alpha = 1.1$ in the PA procedure. Note that as M increases the action level for large R_f/R_m rises and then saturates becoming effectively independent of R_f/R_m . This is presented more precisely in Fig. (4).

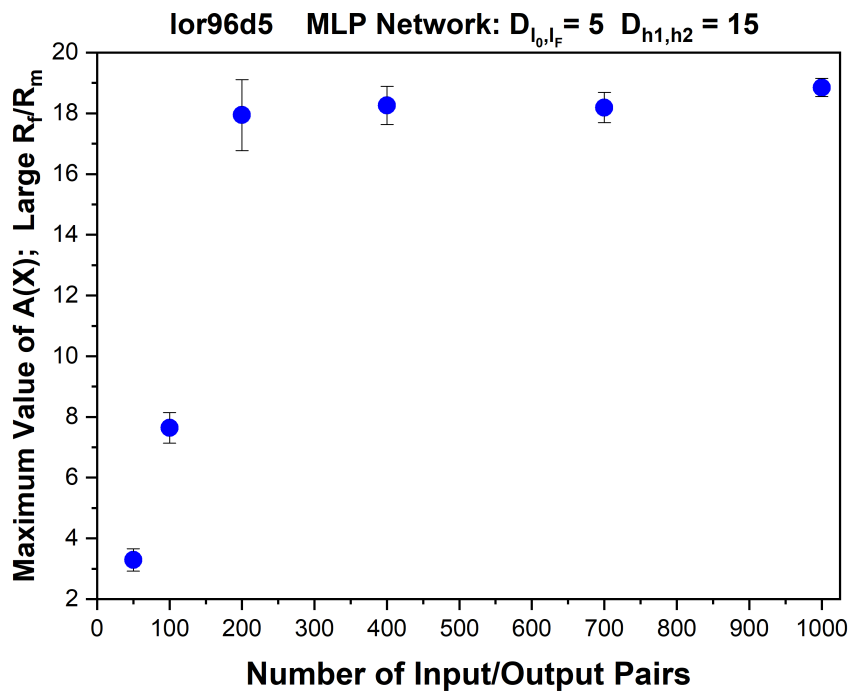


Figure 4: Display of the average and standard deviation of the $N_I = 20$ largest action levels versus the number M of I/O pairs in the training set for our time series $\{s(n)\}$. As seen in the action levels plots as M increases the maximum action levels grow then saturate as the network reaches a full representation of the information in the data pairs. This kind of calculation allows the network designer to determine for a given network architecture how many samples from the I/O library of pairs will be needed to fully train the network. The expected $A(\mathbf{X})$ saturates near $M = 200$.

trained network are the values $\mathbf{Y}^{(k)}(l_0) = \{y(k), y(k+\tau), y(k+2\tau), y(k+3\tau), y(k+4\tau)\}$; the trained network operates on this D_E -dimensional vectors producing the output $x_q^{(k)}(l_F)$; $q = 1, 2, \dots, D_E$. We plot this as a function of M , the number of input/output pairs used in the training procedure, and in Fig. (5) we also examine the dependence on the number of active units (“neurons”) in each of the two hidden layers in the network.

We also can determine the accuracy of the trained network when acting on inputs selected from I/O pairs *not* used in the training of the network. This ‘validation’ error is evaluated as

$$MSE_{\text{Validation Error}}(M) = \frac{1}{M_{\text{total}} - M} \sum_{k=M}^{M_{\text{total}}} \frac{1}{D_E} \sum_{q=1}^{D_E} (x_q^{(k)}(l_F) - y(k+1+(q-1)\tau))^2. \quad (8.2)$$

This compares the D_E -dimensional output $x_q^{(k)}(l_F)$ from the trained network with the data from the set of input/output pairs that **were not used** during the training, $y(k+1+(q-1)\tau)$, that are the output side of the input/output pairs from the data library. We plot this as a function of M , the number of input/output pairs used in the training procedure. All of the I/O pairs from the data library not used in training were used in this validation error estimate. $M_{\text{Total}} = 84971 \gg M$.

In the input layer there are five ports into which a vector $\mathbf{Y}(n) = [y(n), y(n+\tau), y(n+2\tau), \dots, y(n+4\tau)]$ is presented. In each of the hidden layers there are 15 or 25 or 35 active units (‘neurons’). At the output layer there are five ports within which a vector $\mathbf{Y}(n+1) = [y(n+1), y(n+\tau+1), y(n+2\tau+1), \dots, y(n+4\tau+1)]$ is estimated. In Fig. (5) we show the MSEs in the estimation/training window and the prediction/generalization window as a function of the number of active units

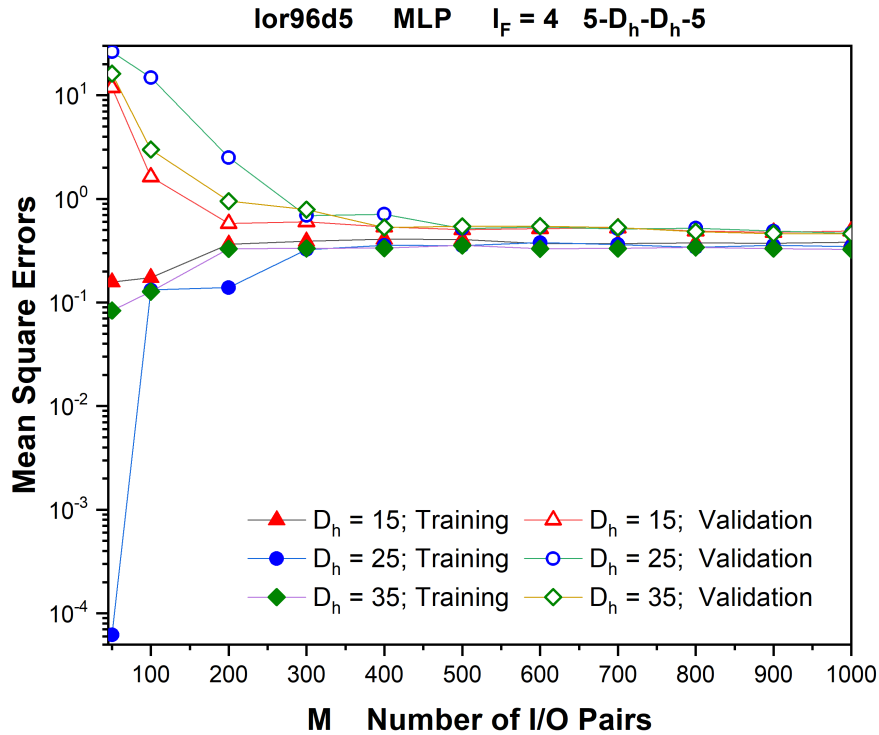


Figure 5: Mean Square Errors (MSE) in the representation of the information in our scalar time series $s(n)$ using a network with four layers. When M is approximately 300, all of these errors become essentially independent of M and very close to being equal. This tells us that to using this network of ‘sigmoids and wires’ we need no more than a few hundred samples of the data to predict as well as we can. No new capability is revealed when M grows beyond that level. This is consistent with the knowledge of the Lyapunov exponents determined for the time series presented to us (Abarbanel, 1996; Kantz & Schreiber, 2003).

D_h in the hidden layers and as a function of the number of input/output pairs M used in training the network. The results show that for small M the training and validation errors differ substantially, but as M increases, enough information lies in the training set of M training I/O pairs that the overall training error levels out when the network has completed its representation of the information in the data. Similarly, while the validation error is large for small M , as the network becomes ‘well trained’ (represents the information in the data series) the prediction MSE is essentially the same as the MSE in training. This result is consistent with the observation that the maximum value of the action levels for large R_f/R_m becomes independent of M ; see Fig.(4).

Fig. (6) examines the training and validation MSEs as a function of the number of layers in the network. The number of hidden layers is $l_F - 2$, and we have evaluated this, using our achitecture, for $l_F = 4, 5$, and 6.

We display the dependence of the action on the number of input/output samples M and R_f/R_m relevant in the PA algorithm in Fig. (7) to further illustrate the outcome of our MLP network instantiation.

In Fig. (8) we display the predictions produced by our trained MLP network after the training using $M = 400$ input/output pairs of segments of the noisy time series starting at $y(n - 1)$ and predicting $y(n)$ in comparison with the known value of $y_{data}(n)$. The training is performed in D_E -dimensional space and the the output of the network is also in D_E dimensional space. We display only the first component of the $D_E = 5$ dimensional proxy state space vector as that is our (noisy) measured quantity. The predictions are what this network has been trained to do.

If we ask another question of the network: take the trained network as a

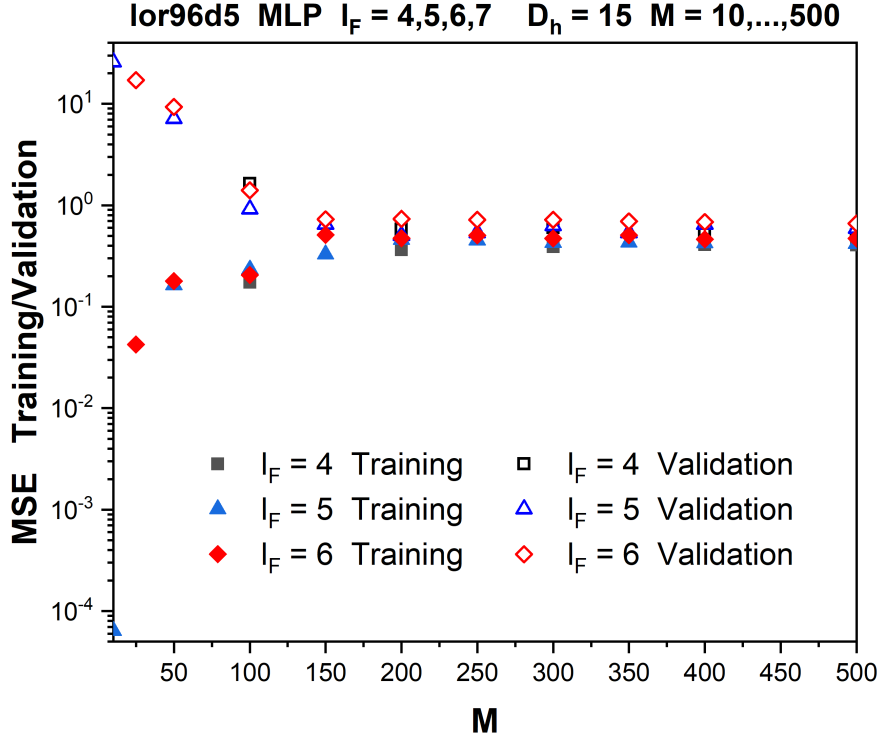


Figure 6: The Mean Square Errors (MSEs) in training and validation (estimation and prediction) for the network architecture with $l_F = 4, 5, 6$ layers. The input and output layers have five ports as before. All hidden layers have 15 active units. We see that when $M \geq 200$ or so, the performance of the network architecture becomes independent of the number of training samples as well as of the number of layers in the network. This result, as in the numerical data displayed in Fig. (5), shows how the PA method can capture the essential information processing power of a selected architecture of a multi-layer perceptron. More to the point, it informs us how many M input/output pairs are required to perform the task set to the machine.

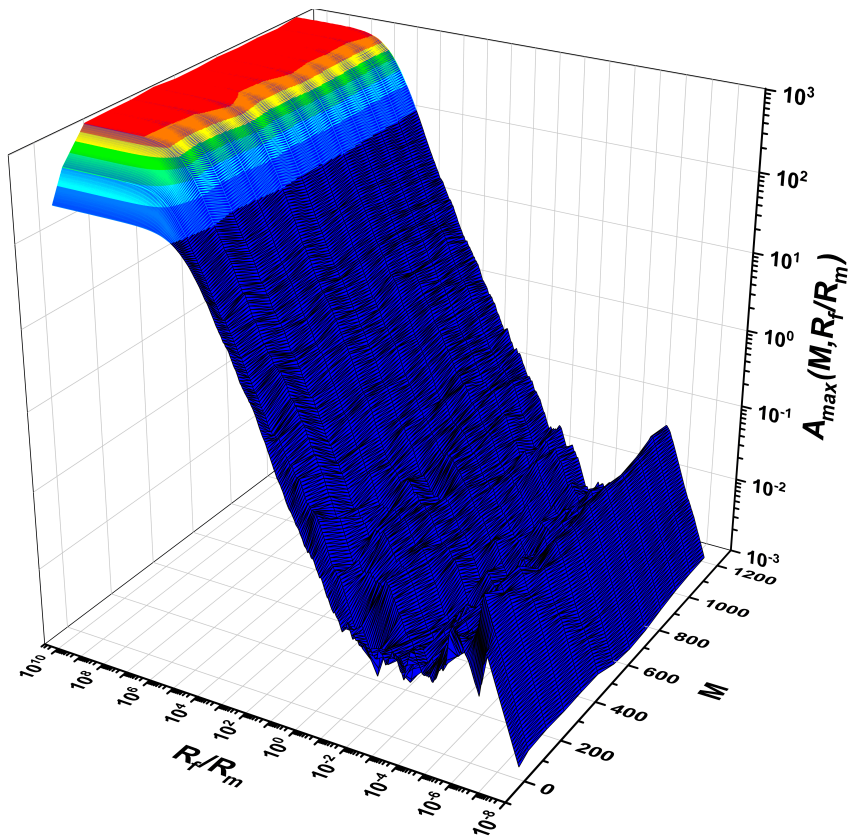


Figure 7: A three dimensional plot of the action for the $l_F = 4$; $D_h = 15$ network as a function of R_f/R_m and the number of input/output pairs M presented for training. It is clear here that a distinct plateau appears in the action, to be thought of as the information content ($-\log[P]$) within the time series data now represented in the network.

dynamical system, namely, train the network using $M = 400$ input output pairs, then use the trained network to predict $y(n) \rightarrow y(n+1)$ forward from the training window, we find the results in Fig. (9). On this task the trained network does not perform as well as on the task it was trained to do

9 Summary and Discussion

Using the interpretation of a familiar machine learning task: using the information flow in a scalar time series to train a rather standard multi-layer perceptron (MLP) to predict one step forward in the time series, as the equivalent of a statistical data assimilation (SDA) task (Abarbanel et al., 2018), we have shown that using the precision annealing (Ye et al., 2014, 2015) training methods of SDA, given the model architecture, leads to a network whose action ($\propto -\log[P(\mathbf{X})]$) rapidly becomes independent of the precision of the model as well as independent of the number M of input/output model pairs and independent of the number of model layers for two or more hidden layers.

We attribute this independence to the class of models having captured the information content within the time series, and thus the method of training reveals how one may use precision annealing to estimate the number of input/output pairs required for excellent training and accurate prediction/generalization. Efforts to this end have been mainly curve-fitting learning curves, for example: (Figuroa, Zeng-Treitler, Kandula, & Ngo, 2012), (Beleites, Neugebauer, Bocklitz, Krafft, & Popp, 2013). Furthermore, as knowledge of the conditional expected values of model state variables is what we wish to utilize approximations of the conditional probability distribution of model states $P(\mathbf{X}|\mathbf{Y})$ for, \mathbf{X} is the collection of all

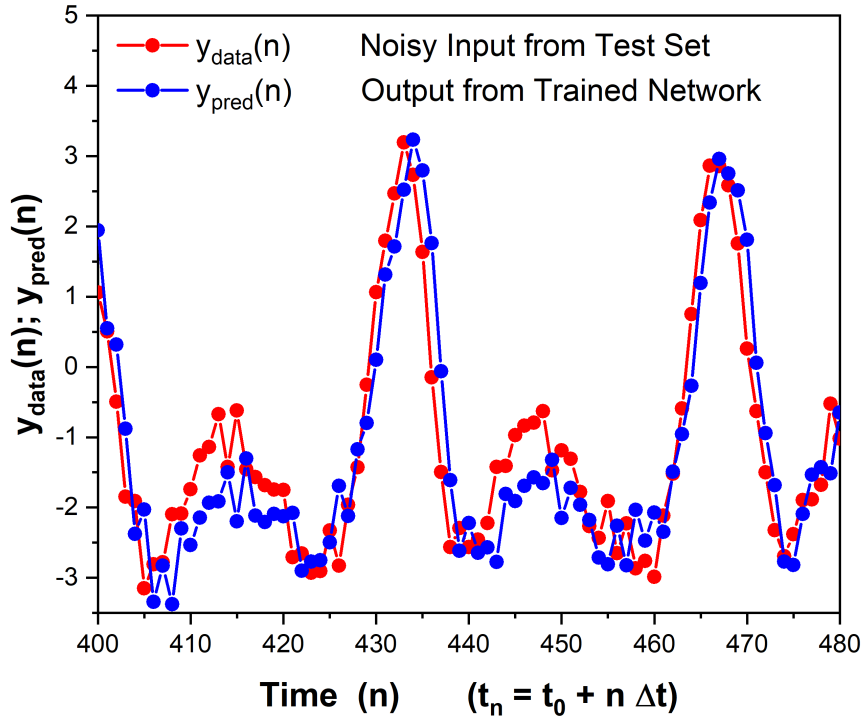


Figure 8: Using the $l_F = 4$; $D_{in} = D_{out} = 5$; $D_h = 15$ network, we show how, after training with 400 pairs of 5 dimensional noisy inputs $\{y(n), \dots, y(n + 4\tau)\}$ and 5 dimensional outputs $\{y(n + 1), \dots, y(n + 4\tau + 1)\}$, this network is able to predict one step ahead for a new five dimensional input.

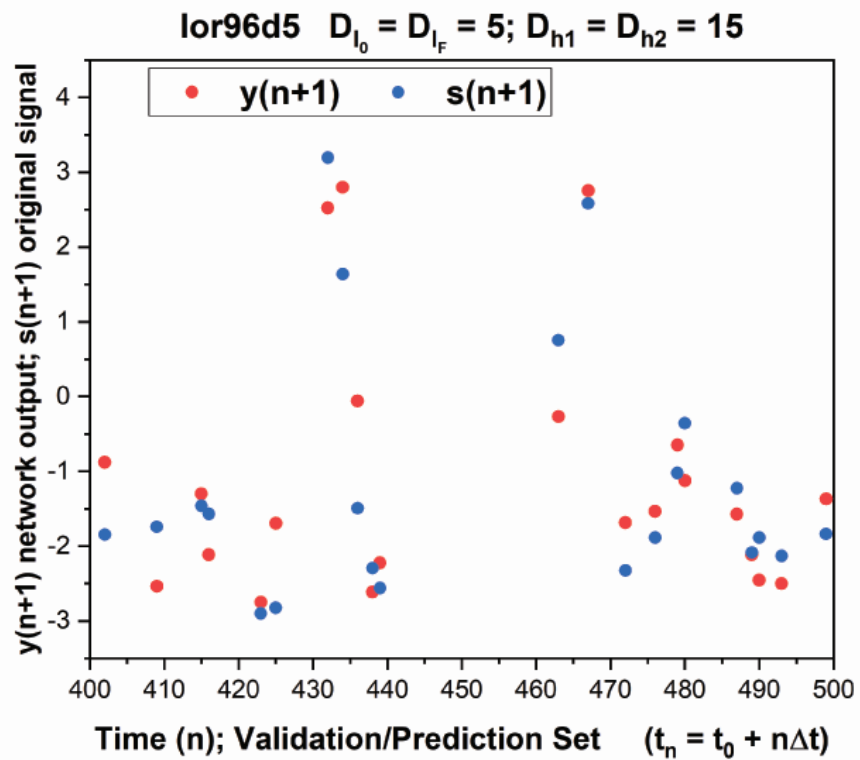


Figure 9: Now we take the trained $l_F = 4; D_{in} = D_{out} = 5; D_h = 15$ network and regard it as a dynamical system taking $s(n) \rightarrow s(n + 1)$. When asked to predict as a dynamical system, namely without continuing information input from the data, the network is not performing well. Of course, the network was not trained to this task.

model states at all layers, and \mathbf{Y} is the collection of all input/output noisy data pairs, we can see how to properly limit the number of data pairs in a training set. This can be important in practical applications.

The data set used in these experiments was generated with the Lorenz96 model equations. Our analysis assumed no knowledge of this to illustrate that the decisions made for preparing the data can be made independent of its source. In curating the data we employed a technique from nonlinear time series analysis (Abarbanel, 1996; Kantz & Schreiber, 2003) that, while well known in the analysis of time series from nonlinear sources, has been used only once (Frank et al., 2001), as far as we could tell, in a machine learning context over some decades. Considering its utility, we employed it here in a bit of detail as a friendly suggestion for future time series investigations.

In our earlier paper (Abarbanel et al., 2018) introducing the analogy between machine learning and SDA, we noted the saturation of actions and prediction quality in a less structured example. We have shown it again here with an attribution to its information theoretic origin. As precision annealing within a Lagrangian training approach from classical methods of variational principles (Gelfand & Fomin, 1963; Marsden & West, 2001; Kadakia, Rey, Ye, & Abarbanel, 2017) is utilized by us, the success may also be attributed to the capability of precision annealing to follow the global minimum of the action even though it is nonlinear in its variables \mathbf{X} (Murty & Kabadi, 1987). This is the value of the action that maximizes the contribution of the conditional expected values of many quantities of interest.

The training method for the MLP network follows that for variational principles in data assimilation (Evensen, 2009; Asch, Bocquet, & Nodet, 2017; Abar-

banel, 2013; Marsden & West, 2001) and control theory (Kirk, 1970; Gelfand & Fomin, 1963) in which ‘backpropagation’ procedures are absent and the methodology is well organized and principled. An additional value of the methods used here and in these references is that the symplectic structure of the variational principles is maintained (Gelfand & Fomin, 1963; Marsden & West, 2001; Kadakia et al., 2017; Abarbanel et al., 2018).

Acknowledgment

Participation by PJR in this research has been partially funded by Deutsche Forschungsgemeinschaft (DFG) through grant CRC 1294 ”Data Assimilation” (project A06).

References

- Abarbanel, H. D. I. (1996). *The analysis of observed chaotic data*. Springer-Verlag, New York.
- Abarbanel, H. D. I. (2013). *Predicting the future: Completing models of observed complex systems*. Springer.
- Abarbanel, H. D. I., & Durstewitz, D. (Fall, 2019). Exploring ‘deepest learning’: Formulation and applications. *online*.
- Abarbanel, H. D. I., Rozdeba, P. J., & Shirman, S. (2018). Machine learning as statistical data assimilation. *Neural Computation*, *30*, 2025-2055.
- Aeyels, D. (1981a). Generic observability of differentiable systems. *SIAM J. Control Optim.*, *19*, 595-603.
- Aeyels, D. (1981b). On the number of samples necessary to achieve observability. *Systems Control Lett.*, *1*, 92-94.
- Allgower, E. L., & Georg, K. (1990). *Numerical continuation methods: An introduction*. Springer-Verlag.
- Asch, M., Bocquet, M., & Nodet, M. (2017). *Data assimilation: Methods, algorithms, and applications*. SIAM.
- Beleites, C., Neugebauer, U., Bocklitz, T., Krafft, C., & Popp, J. (2013, Jan). Sample size planning for classification models. *Anal. Chim. Acta*, *760*, 25–33.
- Evensen, G. (2009). *Data assimilation: The ensemble kalman filter*. Springer.
- Fano, R. M. (1961). *Transmission of information; a statistical theory of communication*. MIT Press.
- Figuroa, R. L., Zeng-Treitler, Q., Kandula, S., & Ngo, L. H. (2012, Feb). Predict-

- ing sample size required for classification performance. *BMC Med Inform Decis Mak*, 12, 8.
- Frank, R. J., Davey, N., & Hunt, S. P. (2001). Time series prediction and neural networks. *Journal of Intelligent and Robotic Systems*, 31, 91-103.
- Fraser, A. M., & Swinney, H. L. (1986). Independent coordinates for strange attractors from mutual information. *Physical Review A*, 35, 1134-1140.
- Gelfand, I. M., & Fomin, S. V. (1963). *Calculus of variations*. Dover Publications, Inc.
- Goodfellow, I., Bengio, Y., & Courville, A. (2016). *Deep learning*. MIT Press, Cambridge, MA; London, UK. Retrieved from <http://www.deeplearningbook.org>
- Kadokia, N., Rey, D., Ye, J., & Abarbanel, H. D. I. (2017). Symplectic methods in statistical data assimilation. *Quarterly Journal of the Royal Meteorological Society*, 143, 756-771.
- Kajitani, Y., Hipel, K. W., & McLeod, A. I. (2005). Forecasting nonlinear time series with feed-forward neural networks: A case study of canadian lynx data. *Journal of Forecasting*, 24, 105-117.
- Kantz, H., & Schreiber, T. (2003). *Nonlinear time series analysis, 2nd ed.* Cambridge University Press, Cambridge, UK.
- Kirk, D. E. (1970). *Optimal control theory: An introduction*. Dover Publications, Inc.
- Laplace, P. S. (1774). Memoir on the probability of causes of events. *Mémoires de Mathématique et de Physique, Tome Sixième*, 621-656.
- Laplace, P. S. (1986). Memoir on the probability of the causes of events. *Statistical Science*, 1(3), 364-378. (Translation to English by S. M. Stigler)

- Marsden, J. E., & West, M. (2001). Discrete mechanics and variational integrators. *Acta Numerica*, 357-514.
- Murty, K. G., & Kabadi, S. N. (1987). Some np-complete problems in quadratic and nonlinear programming. *Mathematical Programming*, 39, 117-129.
- Rozdeba, P. J. (2018). A python package for state and parameter estimation in partially observed ode and neural network systems, using variational annealing. <https://github.com/paulrozdeba/varanneal>.
- Takens, F. (1981). Detecting strange attractors in turbulence. *Lecture Notes in Math.*, 898, 366-381.
- Ye, J., Kadakia, N., Rozdeba, P. J., Abarbanel, H. D. I., & Quinn, J. C. (2014). Improved variational methods in statistical data assimilation. *Nonlinear Processes in Geophysics*, 22(2), 205–213.
- Ye, J., Rey, D., Kadakia, N., Eldridge, M., Morone, U., Rozdeba, P., . . . Quinn, J. C. (2015). A systematic variational method for statistical nonlinear state and parameter estimation. *Physical Review E* 052901.